Scientific paper

Hydrogen Bonds in Bis(1*H*-benzimidazole-κN^3)cadmium(II) Dibenzoate: Hirshfeld Surface Analysis and AIM Perspective

Jia-Jun Wang,[1,2] Li-Nan Dun,[1,2] Bao-Sheng Zhang,[1,2] Zhong-Hui Wang,[3] He Wang,[1,2] Chuan-Bi Li[1,2,*] and Wei Liang[1,2,*]

[1] *Key Laboratory of Preparation and Application of Environmental Friendly Materials, Ministry of Education, Jilin Normal University, Changchun 130103, China*

[2] *Chemistry Department of Jilin Normal University, Siping 136000, China*

[3] *Sulfuric Acid Plant, Jilin Petrochemical Company Acrylonitrile Factory, Jilin 132021, China*

** Corresponding author: E-mail: li_c_b@163.com (Chuan-Bi Li); 16433576@qq.com (Wei Liang)*

Received: 10-09-2020

Abstract

The coordination complex bis(1*H*-benzimidazole-κN^3)cadmium(II) dibenzoate has been synthesized and characterized by single crystal diffraction analysis. Cadmium center is six coordinated and formed a distorted octahedron coordinated geometry. The Hirshfeld analysis shows that in the d_{norm}-surface of the compound, there are dark red spots near the hydrogen-bonds acceptor and donor atoms, while intermolecular interactions result in faint-red spots. The AIM analysis was performed, there exist a BCP in each N(C)–H···O hydrogen bond, the bond paths also can be seen, the $|V(b)|/G(b) < 1$ and the $H(b) > 0$, the interaction is indicative of being a closed shell. The TG results are consistent with the X-ray diffraction structure.

Keywords: Cd Complex, Crystal Structure, TG, Hirshfeld Surface Analysis, AIM Analysis

1. Introduction

Crystal engineering based on coordination complexes[1] have been fast developing in the last few years owing to their potential applications such as absorption,[2] catalysis,[3] luminescence,[4] *etc.* Coordination complexes have already been applied in all aspects of life, and also used for removing the highly toxic heavy metal ions.[5]

The benzimidazoles (Bzim) possess a phenyl ring fused with imidazole ring.[6] Many substances with benzimidazole scaffold have been deeply participated in variety of life activities. For instance, mebendazole is used for treatment of parasitic diseases,[7] and omeprazole is used for gastric ulcers,[8] etc. Many other important properties of metal complexes containing benzimidazoles have also been investigated by researchers. The antibacterial activity of Bzim Zn(II) and Co(II) complexes have been investigated.[9,10] For Bzim's Ir(III) N-heterocyclic carbene complexes' anticancer and antitumor properties were evaluated.[11,12] Bzim derivate's Pt(II) and Cu(II) complexes have DNA binding and/or antioxidant activity.[13,14] Even the Bzim-functionalized ruthenium complexes can be used for dye-sensitized solar cells (DSSC) or energy-storage.[15–17] Thus, exploring the benzimidazole metal coordination complexes is extremely important.

The hydrogen bonds are critical in life science[18] and chemistry.[19] The Hirshfeld surface analysis[20] and the Atom in Molecule (AIM) theory[21] are two powerful tools to research hydrogen bonds from different perspectives. The Hirshfeld sufaces analysis is able to be utilized to identify a type and region of intermolecular interactions (including hydrogen bonds). Hirshfeld surface analyses comprises d_{norm}- and shape index surfaces, and 2D fingerprint plots (FP). While the AIM theory enables us to analyze the properties of hydrogen bonds. In AIM view, the main concept is based on the bond critical point (BCP), they are the evidence of hydrogen bond is the existence of a bond path and a BCP between the donor hydrogen and the acceptor. People also developed the criteria for the assessment of the existence of hydrogen bonds.[22]

In this article, we synthesized a new benzimidazole coordinated cadmium(II) dibenzoate ($Cd(Bzim)_2(BA)_2$

(where Bzim is benzimidazole and BA is benzoate) through the low temperature hydrothermal method, obtained the crystal structure, calculated the molecular orbitals, carried out the Hirshfeld analysis and the AIM analysis, and we mainly focused on the analysis of the hydrogen bonds.

2. Experiments

$Cd(Ac)_2 \cdot 2H_2O$ (0.235 g, 1.0 mmol), benzimidazole (Bzim, 0.236 g, 2.0 mmol), benzoic acid (BA, 0.244g, 2.0 mmol) and 15 mL water were mixed with stirring followed by adjusting the pH value to 6.5 with an aqueous solution of NaOH. Then the mixture was sealed in a 25 mL Teflon-lined stainless-steel reactor and heated at 100 °C for 96 h to give dark yellow crystals of the title compound after cooling. Yield: 32% (based on Cd). IR (cm^{-1}): 3315(w), 3236(w), 1680(s), 1653(s), 1477(s), 1430(s), 1346(w), 877(w), 787(m), 449(m). Anal. Calcd. (%) for $C_{28}H_{22}CdN_4O_4$: C, 56.86; H, 3.72; N, 9.48; Found (%): C, 56.79; H, 3.81; N, 9.53.

3. Structure Determination and Physical Measurements

A yellow block crystal for **1** was chosen for X-ray diffraction analysis. Crystal structure measurement was performed on a Bruker SMART APEX II CCD diffractometer equipped with a graphite-monochromatic Mo*K*α (λ = 0.71073 Å) radiation. Data integration and reduction were performed using SaintPlus 6.01.[23] Absorption corrections were applied with a multi-scan mode.[24] The structure was solved by direct methods with SHELXS[25] and refined by full-matrix least-squares techniques using SHELXL-2018[26] within WINGX.[27] All non-hydrogen atoms were refined anisotropically. All H atoms on C atoms were positioned geometrically and refined as riding, with C–H = 0.93 and $U_{iso}(H) = 1.2U_{eq}(C)$. The molecular graphics was prepared using program Diamond 3.2.[28]

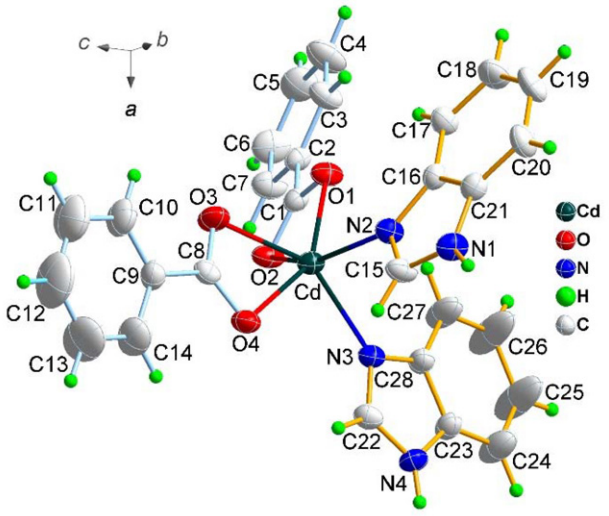

Fig. 1. Molecular structure of $[Cd(Bzim)_2(BA)_2]$, (ellipsoid probability at 30 %).

4. Results and Discussion

4. 1. Structure Description

Table 1. Summary of data collection and structure refinement for the compound.

CCDC	780823
Formula	$C_{28}H_{22}CdN_4O_4$
Formula weight	590.89
Crystal system	Orthorhombic
Space group	*Pbca*
a/Å	14.0359(6)
b/Å	17.7081(8)
c/Å	21.8928(12)
α, b, γ/°	90
V/Å^3	5441.4(5)
Z	8
ρ_{calc}/g cm^{-3}	1.443
Crystal size/mm	0.23×0.20×0.18
F(000)	2384
Reflections collected / unique	37904/6759
R_{int}	0.1203
Data/restraints/parameters	6759 / 0 / 334
Goodness of fit on F^2	0.971
*R*1, *wR*2 (I > 2σ (I))	0.0411, 0.0572
*R*1, *wR*2 (all data)	0.1336, 0.0672
Peak and hole/ e.A^{-3}	0.670, –0.400

A perspective view of the compound, with the atomic numbering scheme, is shown in Fig. **1**. The compound crystallizes in the space group *Pbca* (Table 1). Asymmetric unit consists of a cadmium, two benzimidazole molecules and two benzoic acid ions. The cadmium center is six coordinated and connected four oxygen from two benzoic acids and two nitrogen atoms from two Bzims. Bzim coordinates Cd center in κN coordinate mode and each benzoate ion is bonded to Cd center in a chelating mode. So, the compound can be described as bis(1*H*-benzimidazole-κN^3)cadmium(II) dibenzoate and possess an distorted octahedron geometry.

The Cd–N distances are 2.258(3) and 2.279(3) Å (Table 2), which are not only shorter than the average Cd–$N_{imidazole}$ distance (2.302(3) Å),[29] but also shorter than the Cd–$N_{N\text{-}alkylimidazoles}$ (2.357(2) Å).[30] The Cd–O distances are in the range 2.263(2)–2.490(2) Å, these distances are shorter than the Cd–O distances of the acetate (O_2CMe in chelating mode, 2.294(4)–2.615(3) Å).[31, 32]

The packing diagram is in Fig. 2. In crystal lattice, there are π···π and C-H···π interactions (Table SI). The distances between the center of gravity of the π rings (*Cg*···*Cg* distance) are from 3.68 to 3.97 Å, and the distances between

Table 2. Selected Bond Length and Angles for the Compound.

Bond Length/Angle	Å/º	Bond Angle	º	Bond Angle	º
Cd–N3	2.258(3)	N3–Cd–O1	112.92(10)	O1–Cd–O4	151.39(10)
Cd–O3	2.367(3)	N3–Cd–N2	92.37(10)	N2–Cd–O4	91.57(10)
Cd–O1	2.263(2)	O1–Cd–N2	96.80(10)	O3–Cd–O4	54.82(9)
Cd–O4	2.375(3)	N3–Cd–O3	147.27(10)	N3–Cd–O2	88.65(9)
Cd–N2	2.279(3)	O1–Cd–O3	96.86(9)	O1–Cd–O2	54.60(8)
Cd–O2	2.490(2)	N2–Cd–O3	97.48(10)	N2–Cd–O2	148.68(10)
O4–Cd–O2	119.61(8)	N3–Cd–O4	93.93(10)	O3–Cd–O2	98.43(9)

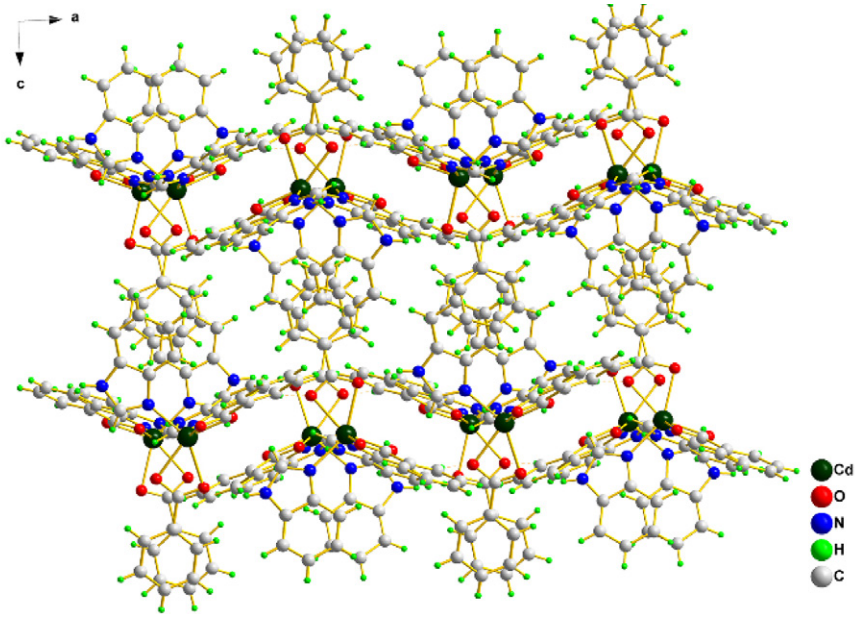

Fig. 2. The packing diagram of the compound.

C atom and *Cg* of the π rings (C···Cg distance) are 3.49 and 3.63 Å. There also exist the N–H···O and C–H···O[33] hydrogen bonds in crystal structure (Table 3), the N···O distances are 2.75 and 2.80 Å, while the C···O distances are 3.21and 3.35 Å. The D–H···A angle of N–H···O (161 and 176°) is larger than the angle of C–H···O (134 and 157°).

Table 3. Hydrogen bonds (Å and °).

Donor-H	Acceptor	D-H	H···A	D···A	D-H···A
N1–H1	O2^{i}	0.86	1.94	2.803(4)	176
N4–H4	O3^{ii}	0.86	1.92	2.748(4)	161
C3–H3	O4^{iii}	0.93	2.47	3.350(4)	157
C22–H22	O1^{ii}	0.93	2.49	3.211(5)	134

Symmetry codes: i = ½ – *x*, ½ + *y*, *z*; ii = ½ + *x*, *y*, ½ – *z*; iii = –½ +*x*, *y*, ½ – *z*.

4. 2. Hirshfeld Surface Analysis

In the last few years the analysis of molecular crystal structures using tools based on Hirshfeld surfaces has rapidly gained in popularity,[34–36] and they were carried out and plotted using CrystalExplorer software.[20,37–41] Hirshfeld surface analysis comprising d_{norm}- and shape index-surfaces, and 2D fingerprint plots (FP).

In d_{norm}-surface, hydrogen-bonds result in dark red spots near the hydrogen-bonds acceptor and donor atoms while intermolecular interactions result in faint-red spots. Further, the presence of patterns of red- and blue triangles on the same region of the shape-index surfaces is characteristic of π···π stacking. The d_{norm}- and shape index-surfaces of the compound are shown in Fig. 3 and Fig. 4.

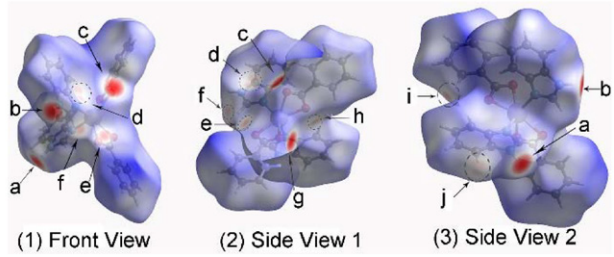

Fig. 3. The d_{norm} surfaces of the compound.

The N–H···O hydrogen-bonds in title compound can be seen in the d_{norm}-surfaces as bright-red spots marked as *a, b, c* and *g* (the spots located near the atom each correspondence are: *a* → N1, *b* → N4, *c* → O2, *g* → O3) in Fig. 3, so that the *a*, *b*, *c* and *g* spots are due to N1–H1···O2 and N4–H4···O3 hydrogen bonds.

The weak C–H···O hydrogen bond interactions (including intramolecular and intermolecular hydrogen bonds) in the compound are also demonstrated in the d_{norm}-surface as faint-red color spots (Fig. 3) and signed as *e, f, h, i*. (that is, each correspondence are: *e* → O4, *f* → C22, *h* → O1, *i* → C3). The faint-red spots above the center of the benzimidazole ring in the d_{norm}-surface of the compound (Fig. 3), all marked as *d*, arise from the C20–H20···π(Cg5) and C20–H20···π(Cg6) interaction, observed in crystal structure. The offset π···π interactions observed in the crystal structure are identified by distinctive patterns of red- and blue-triangles across the respective phenyl rings on the shape-index surface plots of the molecule (see the circle in Fig. 4).

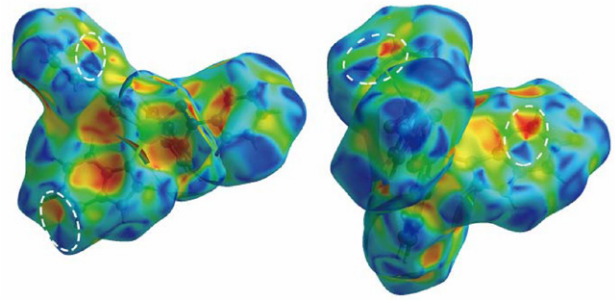

Fig. 4. The shape-index-surfaces.

The quantitative analysis of the intermolecular interactions apparent in crystal structure was attempted by observing the 2D FP's (Fig. 5). The H···O intermolecular interactions in the compound, appeared as two distinct long sharp spikes in the FP, at $d_i + d_e \approx 1.75$ Å which is roughly close to the observed N1–H1···O2 and N4–H4···O3 distance of 1.92, 1.94 Å (Table 3). In one molecule, these two spikes appear at (d_i, d_e) ≈ (0.70 Å, 1.05 Å) and (d_e, d_i) ≈ (0.70 Å, 1.05 Å, Fig. 5d), and the spikes appear in the same manner.

The C–H···π interactions appear as pair of blunt spikes at (d_e, d_i) ≈ (1.78 Å, 1.0 Å) and (d_e, d_i) ≈ (1.0 Å, 1.78 Å) in the FP, occurring at $d_i + d_e \approx 2.78$ Å, it appear as the spikes at $d_i + d_e$ distances are close to the H···π(Cg) distances in crystal (2.57, 2.80 Å, Table SI, Fig.5 (c)). The C–H···π interactions (Table SI) are also supported by the 'two wings' characters,[39–41] the wings are sites at the upper left and the bottom right. For the C···C close contacts (Fig. 5 (e)) with the shortest $d_i + d_e$ (distances ≈ 1.73 + 1.73 = 3.46 Å) is roughly accord with the C···C distances 3.68–3.97 Å in Table SI. It corresponds to the π···π stacking interactions.

The relative contributions of the intermolecular interactions to the Hirshfeld surface for the compound was calculated (see the upper bar diagram in Fig. 5(g)). The greatest contribution (47.2%) is from H···H contacts, followed by H···C/C···H contacts (which is stands for the C-H···π intermolecular interactions, 27.4%), then is the H···O/O···H contacts (the C-H···O or N-H···O hydrogen bond interactions 14.0%), the contribution from the H···N/N···H contacts is 4.2%, other contacts is 1.1%.

4. 3. Atom in Molecules Analysis

The topology analysis proposed by Bader was initially used for researching electron density in "atoms in

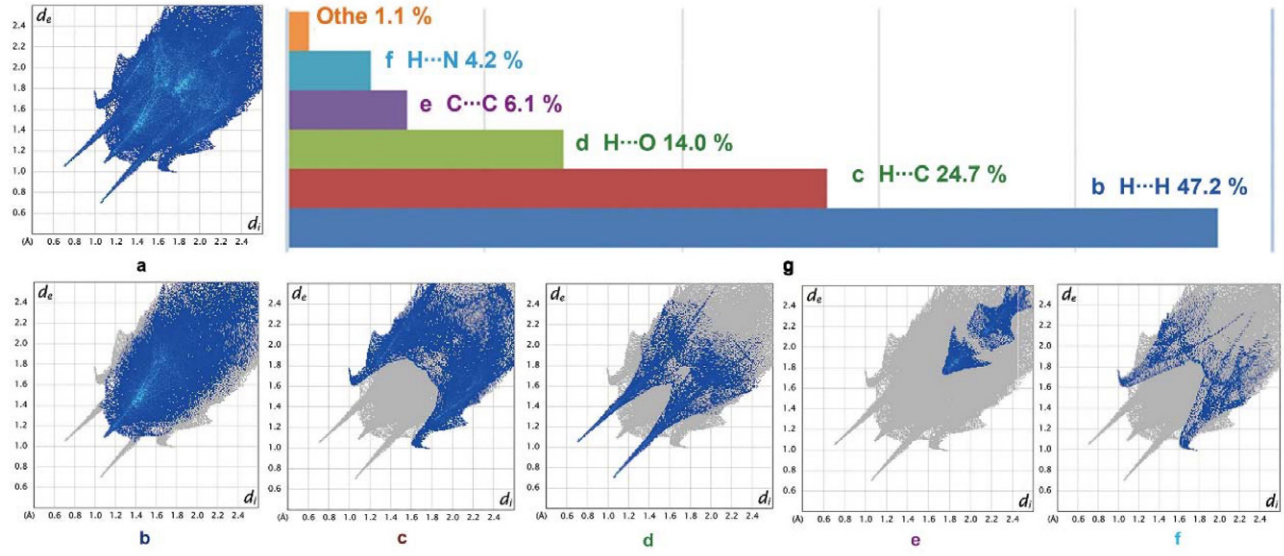

Fig. 5a The full image of Fingerprint Plot. **Fig. 5b** The H···H contacts show the contribution of 47.2%. **Fig. 5c** The H···C contacts have a contribution of 24.7%. **Fig. 5d** The H···O contacts have a contribution of 14.0% which is manifested by the interactions due to hydrogen bonds of N–H···O and C-H···O type. **Fig. 5e** The C···C contacts display the contribution of 6.1%. **Fig. 5f** The H···N contacts exhibit the contribution of 4.2%. **Fig. 5g** The bar graph shown the proportion of each contacts.

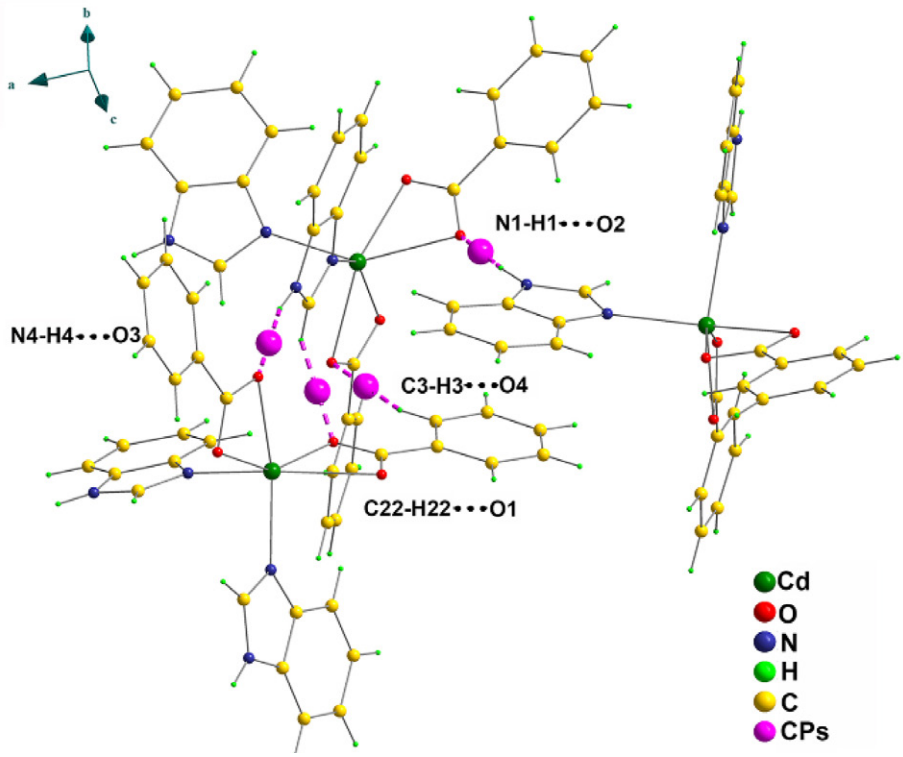

Fig. 6. The general view of hydrogen bonds BCP (pink ball) from the three coordinated unit model of the compound.

molecules" (AIM) theory.[21,42,43] In this theory, based on the bond critical point (BCP), Popelier[22] proposed the hydrogen bond's electron density at the BCP (ρ_{BCP}) should be in the scope of 0.002–0.035 a.u. and the electron density Laplacian value ($\nabla^2\rho_{BCP}$) should be confined in the region from 0.024 to 0.139 a.u.

For investigating the hydrogen bonds, we select three coordination units to form the model (it contain three molecules), in which it can exhibit the hydrogen bonds and the π···π interactions from the cif file (see supporting information) and calculate the single point to get the fchk file (see supporting information) from Gaussian 09 program[44] at ωB97XD[45]/GenECP (6-31+G** basis set for C, H, O, N and Lanl2dz[46] basis set for Cd), finally, we use the Multiwfn program[47] to study the topological properties of the hydrogen bonds in title compound (The Multiwfn produced CPs.pdb, Path.pdb and CPprop.txt are also in supporting information).

Fig. 6 shows the existence of a BCP in each N–H···O and each C–H···O hydrogen bond. The bond paths associated with the hydrogen bonds can be seen in Fig. 5 (and also be seen in Fig. S1). The BCP electron density of the hydrogen bonds is listed in Table 4. The ρ_{BCP} value (from 0.009 to 0.032 a.u.) for the N–H···O and C–H···O hydrogen bonds are all in the suggested interval of 0.002–0.035 a.u.[48] for the hydrogen bond. The two negative Hessian matrix eigenvalues of electron density, λ_1 and λ_2, can measure the scope of contraction of ρ_{BCP} which is perpendicular to the bond toward the critical point, while the positive λ_3 eigenvalue weighs the extent of contraction parallel to the bond and from the BCP toward each of the adjacent nuclei. The sum of eigenvalues λ_1, λ_2, and λ_3 is $\nabla^2\rho_{BCP}$. In addition, the numeric value of $\nabla^2\rho_{BCP}$ (0.0322–0.1091 a.u.) for N(C)–H···O interactions are in the recommend region of 0.024–0.139 a.u. for hydrogen bonds. Bader et al. deemed that for the closed-shell interactions (including

Table 4. The electron density (ρ_{BCP}), the Laplacian of electron density ($\nabla^2\rho_{BCP}$), and the eigenvalues of Hessian at BCP (λ_1, λ_2 and λ_3)[a]. Computed at ωB97XD/GenECP Level (6-31+G(d) for C, H, O, N and LanL2DZ for Cd).

Interactions	ρ_{BCP}	$\nabla^2\rho_{BCP}$	λ_1	λ_2	λ_3
N1–H1···O2	0.0324	0.1091	−0.0458	−0.0456	0.2006
N4–H4···O3	0.0254	0.0950	−0.0320	−0.0326	0.1596
C3–H3···O4	0.0093	0.0322	−0.0086	−0.0092	0.0500
C22–H22···O1	0.0091	0.0343	−0.0087	−0.0080	0.0510

a – The unit is atom unit.

the ionic bonds, hydrogen bonds, and van der Waals interactions) the $\nabla^2\rho_{BCP}$ value is positive.[21,43,49–54] On the basis of Table 4, the N–H···O and C–H···O hydrogen bonds are typical closed-shell interactions. Clearly, the topological properties of the hydrogen bonds studied are closed-shell interactions.

Table 5 The local properties at BCP: the potential energy density, V(b); the Lagrangian kinetic energy density, G(b); and the total energy density H(b)[a]. The calculations at ωB97XD/GenECP level (6-31+G(d) for C, H, O, N and LanL2DZ for Cd).

Interactions	V(b)	G(b)	H(b)	|V(b)|/G(b)
N1–H1···O2	–0.02476	0.02602	0.00126	0.92158
N4–H4···O3	–0.02100	0.02237	0.00137	0.93876
C3–H3···O4	–0.00655	0.00731	0.00075	0.89603
C22–H22···O1	–0.00622	0.00740	0.00116	0.84054

a – The unit is atom unit (a.u.).

Morrison,[55] and Espinosa[56] et al.[57] suggested that bond interactions are sorted according to the $|V(b)|/G(b)$ ratio, the ratio $|V(b)|/G(b) < 1$, the bonded interaction is taken for the closed shell, when $|V(b)|/G(b) > 2$, it is typically covalent interaction; and when $1 < |V(b)|/G(b) < 2$, it is the intermediate character. As it is depicted in Table 5, the Lagrangian kinetic energy density is only slightly larger than the potential energy density for all the (N)C–H···O interactions. It brings about the total energy density $H(b)$ is drawn near to 0 and the $|V(b)|/G(b)$ ratio is a little less than 1.0. Consequently, the N(C)–H···O interactions are mainly the closed shell for the model of the compound. This conclusion is agreement with the $\nabla^2\rho_{BCP} > 0$.

4. 4. Thermogravimetric Analysis

The TG of the title compound at the heating rate of 10 °C/min in nitrogen atmosphere is shown in Fig. 7.

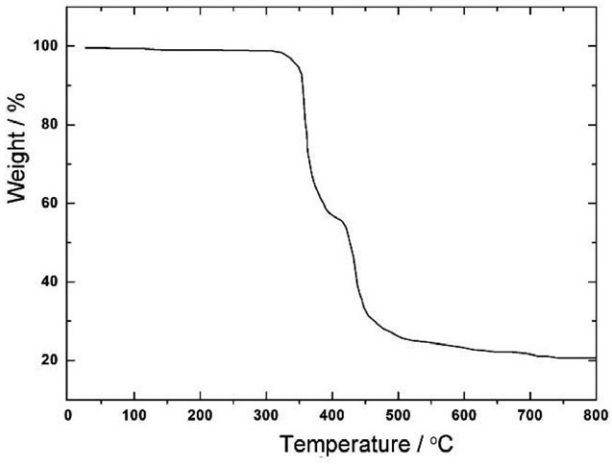

Fig. 7. The TG Analysis of the Compound.

There are two weight loss steps. The first weight loss stage mainly takes place from 301 to 393 °C, it may be related to the removal of the coordinated benzimidazole molecules (found: 41.14%; calcd: 39.99%). The second weight loss step mainly takes place from 405 to 636 °C, it corresponds to the release of the coordinated benzoate anion (found: 36.3%, calcd.: 40.99%). After 650 °C, nearly no weight loss is observed and the residue weight is 20.59%, which suggests it may be the cadmium oxide (CdO, calcd.: 21.73%).

5. Conclusion

The coordination complex bis(1*H*-benzimidazole-κN^3)cadmium(II) dibenzoate has been synthesized, the crystal structures were characterized by the single crystal diffraction analysis, Hirshfeld analysis and the AIM analysis. The structure analysis reveals that the cadmium center is six coordinated and forms an distorted octahedron coordinated geometry, and the compound's formula is $Cd(Bzim)_2(C_6H_5COO)_2$. The Hirshfeld analysis shows that in the d_{norm}-surface, there are dark red spots near the hydrogen-bond acceptor and donor atoms, while intermolecular interactions result in faint-red spots, the offset π···π interactions observed are identified by distinctive patterns of red- and blue-triangles across the respective phenyl rings on the shape-index surface plots, and the 2D fingerprint plots were also investigated. The AIM analysis shows there exists a BCP in each N–H···O and each C–H···O hydrogen bond, the bond paths associated with the hydrogen bonds can be seen, and the $|V(b)|/G(b) < 1.0$ and the $H(b) > 0$, these results manifested that the interaction is a closed shell system. The TG plot shows two weight loss steps (corresponding to BA and Bzim), the residue may be the cadmium oxide (CdO).

Acknowledgments

Supported by the Project of the Education Department of Jilin Province, China (No. JJKH20180777KJ) and the Science and Technology Development Projects of Siping City (No. 2017057).

6. References

1. S. R. Batten, N. R. Champness, X. M. Chen, J. Garcia-Martinez, S. Kitagawa, L. Öhrström, M. O'Keeffe, M. P. Suh, J. Reedijk, *Pure Appl. Chem.* **2013**, *85*, 1715–1724. **DOI:**10.1351/PAC-REC-12-11-20
2. P. García-Holley, B. Schweitzer, T. Islamoglu, Y. Y. Liu, L. Lin, S. Rodriguez, M. H. Weston, J. T. Hupp, D. A. Gómez-Gualdrón, T. Yildirim, O. K. Farha, *ACS Energy Lett.* **2018**, *3*, 748–754. **DOI:**10.1021/acsenergylett.8b00154
3. H. Kaur, M. Venkateswarulu, S. Kumar, V. Krishnana, R. R.

Koner, *Dalton Trans.* **2018**, *47*, 1488–1497. **DOI:**10.1039/C7DT04057A
4. Y. Rachuri, B. Parmar, E. Suresh, *Cryst. Growth Des.* **2018**, *18*, 3062–3072. **DOI:**10.1021/acs.cgd.8b00204
5. H. R. Wang, W. Meng, J. Wu, J. Ding, H. W. Hou, Y. T. Fan, *Coord. Chem. Rev.* **2016**, *307*, 130–146. **DOI:**10.1016/j.ccr.2015.05.009
6. M. Faheem, A. Rathaur, A. Pandey, V. K. Singh, A. K. Tiwari, *ChemistrySelect* **2020** *5*, 3981–3994. **DOI:**10.1002/slct.201904832
7. R. Cañete, A.A. Escobedo, P. Almirall, M.E. González, K. Brito, S. Cimerman, *Trans. R. Soc. Trop. Med. Hyg.* **2009**, *103*, 437–442. **DOI:**10.1016/j.trstmh.2008.11.029
8. L. Witzel, H. Gütz, W. Hüttemann, W. Schepp, *Aliment. Pharmacol. Ther.* **1995**, *9*, 19–24. **DOI:**10.1111/j.1365-2036.1995.tb00346.x
9. K. Chkirate, K. Karrouchi, N. Dege, N. K. Sebbar, A. Ejjoummany, S. Radi, N. N. Adarsh, A. Talbaoui, M. Ferbinteanu, E. M. Essassia, Y. Garcia, *New J. Chem.* **2020**, *44*, 2210–2221. **DOI:**10.1039/C9NJ05913J
10. S. O. Podunava-Kuzmanovi, D. M. Cvetkovi, *J. Serb. Chem. Soc.* **2007**, *72*, 459–466. **DOI:**10.2298/JSC0705459P
11. Y. Han, X. Liu, Z. Tian, X. Ge, J. Li, M. Gao, Y. Li, Y. Liu, Z. Liu. *Chem.-Asian J.* **2018**, *13*, 3697–3705. **DOI:**10.1002/asia.201801323
12. X. Liu, Y. Han, X. Ge, Z. Liu, *Front. Chem.* **2020**, *8*, 182. **DOI:**10.3389/fchem.2020.00182
13. Ö. Tarı, F. Gümüsß, L. Açık, B. Aydın, *Bioorg. Chem.* **2017**, *74*, 272–283. **DOI:**10.1016/j.bioorg.2017.08.015
14. H. Wu, F. Kou, F. Jia, B. Liu, J. Yuan, Y. Bai, *Bioinorg. Chem. Appl.* **2011**, 105431. **DOI:**10.1155/2011/105431
15. M. Tercan, O, Dayan, *J. Electron. Mater.* **2019**, *48*, 642–648. **DOI:**10.1007/s11664-018-6758-8
16. W. K. Huang, C. W. Cheng, S. M. Chang, Y. P. Lee, E. W. G. Diau, *Chem. Commun.* **2010**, *46*, 8992–8994. **DOI:**10.1039/c0cc03517c
17. D. Motoyama, K. Yoshikawa, H. Ozawa, M. Tadokoro, Masa-aki Haga, *Inorg. Chem.* **2017**, *56*, 6419–6428. **DOI:**10.1021/acs.inorgchem.7b00518
18. G. A. Jeffrey, W. Saenger, Hydrogen Bonding in Biological Structures. Springer, 1991.pp 169–464. **DOI:**10.1007/978-3-642-85135-3
19. K. Choi, A. D. Hamilton, *Coord. Chem. Rev.* **2003**, *240*, 101–110. **DOI:**10.1016/S0010-8545(02)00305-3
20. S. K. Seth, D. Sarkar, A. D. Jana, T. Kar, *Cryst. Growth Des.* **2011**, *11*, 4837–4849. **DOI:**10.1021/cg2006343
21. R. F. W. Bader, T. S. Slee, D. Cremer, E. Kraka, *J. Am. Chem. Soc.*, **1983**, *105*, 5061–5068. **DOI:**10.1021/ja00353a035
22. P. L. A. Popelier, *J. Phys. Chem. A* **1998**, *102*, 1873–1878. **DOI:**10.1021/jp9805048
23. Bruker, *SAINT-V6.28A Data Reduction Software*, Bruker AXS Inc., Madison, WI, USA, **2001**.
24. T. Higashi, *Program for Absorption Correction*. Rigaku Corporation, Tokyo, Japan, **1995**.
25. G. M. Sheldrick, *Acta Cryst.* **2008**, *A64*, 112–122. **DOI:**10.1107/S0108767307043930
26. G. M. Sheldrick, Acta Cryst. (2015). C71, 3–8. **DOI:**10.1107/S2053229614024218
27. L. J. Farrugia, *J. Appl. Cryst.* **2012**, *45*, 849–854. **DOI:**10.1107/S0021889812029111
28. H. Putz, K. Brandenburg, Diamond - Crystal and Molecular Structure Visualization Crystal Impact - Brandenburg GbR, Kreuzherrenstr. 102, 53227 Bonn, Germany, http://www.crystalimpact.com/diamond
29. G. C. Liu, J. X. Zhang, X. L. Wang, H. Y. Lin, A. X. Tian, Y. F. Wang, *Z. Naturforsch*. **2011**, *66b*, 125–132. **DOI:**10.1515/znb-2011-0204
30. E. A. H. Griffith, N. G. Charles, E. L. Amma, *Acta Cryst. Sect. B* **1982**, *38*, 942–944. **DOI:**10.1107/S0567740882004518
31. J. Ryu, G. M. Lee, S. W. Lee, *Bull. Korean Chem. Soc.* **2019**, 40, 958–962. **DOI:**10.1002/bkcs.11853
32. W. Harrison, J. Trotter, *J. Chem. Soc. Dalton Trans.* **1972**, 956–960. **DOI:**10.1039/dt9720000956
33. T. Steiner, *Cryst. Rev.* **1996,** *6*, 1–57. **DOI:**10.1080/08893110310001621772
34. L. Bejaoui, J. Rohlíček, V. Eigner, A. Ismail, M. E. Bour, R. B. Hassen, *Acta. Chim. Slov.* **2019**, 66, 603–613. **DOI:**10.17344/acsi.2019.5002
35. R. Vafazadeh, Z. Mansouri, A. C. Willis, *Acta. Chim. Slov.* **2020**, 67, 516–521. **DOI:**10.17344/acsi.2019.5539
36. L. Bejaoui, J. Rohlicek, R. B. Hassen, *J. Mol. Struct.* **2018**, 1173, 574e582. **DOI:**10.1016/j.molstruc.2018.07.017
37. M. A. Spackman, D. Jayatilaka. *Cryst. Eng. Comm.* **2009**, *11*, 19–32. **DOI:**10.1039/B818330A
38. M. J. Turner, J. J. McKinnon, S. K. Wolff, D. J. Grimwood, P. R. Spackman, D. Jayatilaka and M. A. Spackman, CrystalExplorer17, University of Western Australia. 2017. http://hirshfeldsurface.net
39. M. A. Spackman, P. G. Byrom, *Chem. Phys. Lett.* **1997**, *267*, 215–220. **DOI:**10.1016/S0009-2614(97)00100-0
40. J. J. McKinnon, A. S. Mitchell, M. A. Spackman, *Chem. Eur. J.* **1998**, *4*, 2136–2141. **DOI:**10.1002/(SICI)1521-3765(19981102)4:11<2136::AID-CHEM2136>3.0.CO;2-G
41. J. J. McKinnon, M. A. Spackman, A. S. Mitchell, *Acta Crystallogr., Sect. B* **2004**, *60*, 627–668. **DOI:**10.1107/S0108768104020300
42. R. F. W. Bader, *Acc. Chem. Res.* **1985**, *18*, 9–15. **DOI:**10.1021/ar00109a003
43. R. F. W. Bader, *Chem. Rev.* **1991**, *91*, 893–928. **DOI:**10.1021/cr00005a013
44. M. J. Frisch, G. W. Trucks, H. B. Schlegel, G. E. Scuseria, M. A. Robb, J. R. Cheeseman, G. Scalmani, V. Barone, B. Mennucci, and D. J. Fox, et.al. Gaussian 09, Revision D.01, Gaussian, Inc., Wallingford CT, 2009.
45. J. D. Chai, M. Head-Gordon, *Phys. Chem. Chem. Phys.* **2008**, *10*, 6615–6620. **DOI:**10.1039/b810189b
46. P. J. Hay, W. R. Wadt, *J. Chem. Phys.* **1985**, *82*, 270–283. **DOI:**10.1063/1.448799
47. T. Lu, F. W. Chen, *J. Comp. Chem.* **2012**, *33*, 580–592. **DOI:**10.1002/jcc.22885
48. U. Koch, P. Popelier, *J. Phys. Chem.* 1995, *99*, 9747–9754. **DOI:**10.1021/j100024a016

49. R. F. W. Bader, *J. Phys. Chem. A* **1998**, *102*, 7314–7323. **DOI:**10.1021/jp981794v
50. F. Biegler-König, R. F. W. Bader, T.H. Tang, *J. Comput. Chem.* **1982**, *3*, 317–328. **DOI:**10.1002/jcc.540030306
51. T. H. Tang, R. F.W. Bader, P. MacDougall, *Inorg. Chem.* **1985**, *24*, 2047–2053. **DOI:**10.1021/ic00207a018
52. F. Biegler-König, J. Schonbohm, D. Bayles, *J. Comput. Chem.* **2001**, *22*, 545–559. **DOI:**10.1002/1096-987X(20010415)22:5<545::AID-JCC1027>3.0.CO;2-Y
53. F. Biegler-König, J. Schonbohm, *J. Comput. Chem.* **2002**, *23*, 1489–1494. **DOI:**10.1002/jcc.10085
54. R. F. W. Bader, Atoms in Molecules–A Quantum Theory, Oxford University Press, New York, 1990, pp. 290–315.
55. S. Jenkins, I. Morrison, *Chem. Phys. Lett.* **2000**, *317*, 97–102. **DOI:**10.1016/S0009-2614(99)01306-8
56. E. Espinosa, I. Alkorta, J. Elguero, E. Molins, *J. Chem. Phys.* **2002**, *117*, 5529–5542. **DOI:**10.1063/1.1501133
57. S. Dinda, A. G. Samuelson, *Chem. Eur. J.* **2012**, *18*, 3032–3042. **DOI:**10.1002/chem.201101219

Povzetek

Sintetizirali smo koordinacijsko spojino bis(1*H*-benzimidazol-κN^3)kadmijev(II) dibenzoat in ga okarakterizirali z rentgensko monokristalno analizo. Kadmijev center je heksakoordiniran s popačeno oktaedrično geometrijo. Hirshfeldova analiza razkrije, da so na površini d_{norm} temno rdeče točke blizu akceptorjev in donorjev vodikovih vezi, medtem ko bledordeče točke predstavljajo intermolekularne interakcije. AIM analiza pokaže, da so BCP pri vsaki N(C)–H···O vodikovi vezi, |V(b)|/G(b) < 1 in H(b) > 0 pa nakazujeta na closed shell interakcijo. TG analiza potrjuje kristalno strukturo.